

RESEARCH ARTICLE OPEN ACCESS

# Forcing the Side-on $\pi$ -Coordination of a $C\equiv C$ Triple Bond to Technetium Using the $As,CC,As$ Alkyne Pincer Ligand 1,2-Bis(2-(diisopropylarsanyl)-4-(trifluoromethyl)phenyl)Ethyne

 Maximilian Roca Jungfer<sup>1</sup>  | Moritz Johannes Ernst<sup>2</sup>  | Lukas Eberle<sup>3</sup>  | Marius Kesselring<sup>2,4</sup>  |  
 Guilhem Claude<sup>4</sup>  | Joachim Ballmann<sup>3</sup> 

<sup>1</sup>Institut Für Nukleare Entsorgung (INE), Karlsruher Institut für Technologie (KIT), Eggenstein-Leopoldshafen, Germany | <sup>2</sup>Fachbereich Biologie, Chemie, Pharmazie, Institut Für Anorganische Chemie, Freie Universität Berlin, Berlin, Germany | <sup>3</sup>Anorganisch Chemisches Institut, Ruprecht-Karls-Universität Heidelberg, Heidelberg, Germany | <sup>4</sup>Corporate Member of Freie Universität Berlin and Humboldt Universität Zu Berlin, Klinik für Nuklearmedizin/Radiopharmazie, Charité – Universitätsmedizin Berlin, Berlin, Germany

**Correspondence:** Maximilian Roca Jungfer ([maximilian.roca-jungfer@partner.kit.edu](mailto:maximilian.roca-jungfer@partner.kit.edu); [m.roca.jungfer@gmail.com](mailto:m.roca.jungfer@gmail.com))

**Received:** 29 January 2026 | **Revised:** 23 March 2026 | **Accepted:** 27 March 2026

**Keywords:** <sup>99m</sup>Tc | alkyne | radioactive | side-on | technetium

## ABSTRACT

Alkyne complexes are known for transition metals across the d-block with exception of the radioelement technetium despite considerable synthetic efforts. DFT calculations suggest that this is not inherent to the transition metal but a consequence of the overall ligand sphere. The arsenic-based tolane ligand 1,2-bis(2-(diisopropylarsanyl)-4-(trifluoromethyl)phenyl)ethyne ( $L^{iPr}$ ) forces a coordination of the central alkyne moiety onto the metal through ligand design. The stable, crystalline Tc(III) and Tc(V) alkyne complexes  $mer-[Tc^{III}Cl_3(\chi^4-As,CC,As-L^{iPr})]$ ,  $mer-[Tc^VNX_2(\chi^4-As,CC,As-L^{iPr})]$  ( $X = Cl, Br$ ) and  $cis,trans,mer-[Tc^VN(CN)Cl(\chi^4-As,CC,As-L^{iPr})]$  alongside their rhenium homologs  $mer-[Re^VCl_3(\chi^4-As,CC,As-L^{iPr})]$  and  $mer-[Re^VNCl_2(\chi^4-As,CC,As-L^{iPr})]$  have been prepared and fully characterized. According to spectroscopic and DFT analyses, the technetium complexes represent robust, classical  $2e^-$  alkyne complexes, while a different situation was found for  $mer-[Re^VCl_3(\chi^4-As,CC,As-L^{iPr})]$  with a formally oxidized metal ion and reduced  $4e^-$  donor ligand. This has general implications for  $\pi$ -ligand coordination in group 7 and potentially for neighboring elements. Successful translation to the medically relevant nuclear isomer <sup>99m</sup>Tc proves the viability of alkyne donors as building blocks for stable chelation of technetium at the tracer level.

## 1 | Introduction

Since their discovery, alkyne complexes have been isolated for all but one element of the central d-block: the artificial radioelement technetium [1–6]. This is not only especially surprising given the abundance, ease of formation, and structural variety of alkyne complexes containing the heavier homolog of technetium, rhenium (examples in references) [7–32], which often resembles technetium in its chemistry but also contrasts with the behavior

of other neighboring elements in the periodic table (Figure 1 [1–6, 33, 34], for additional information see S5.1, S5.11).

Probing the coordination of alkynes to technetium is therefore of fundamental interest to organometallic chemistry [1–6], also considering that an  $\pi$ - $\eta^2$ -alkene and  $\pi$ - $\eta^2$ -nitrile have been isolated in traces inadvertently [35, 36], and some arene or cyclopentadienyl  $\pi$ -complexes are known [1, 37, 38]. Plentiful attempts to bind alkyne ligands to technetium have been made

This is an open access article under the terms of the [Creative Commons Attribution](https://creativecommons.org/licenses/by/4.0/) License, which permits use, distribution and reproduction in any medium, provided the original work is properly cited.

© 2026 The Author(s). *Angewandte Chemie International Edition* published by Wiley-VCH GmbH

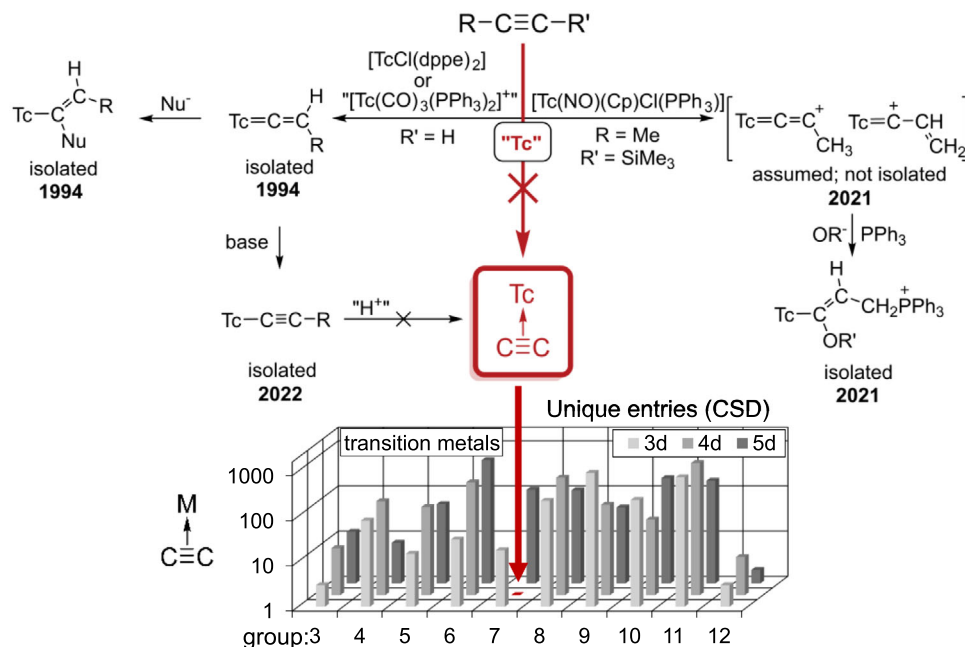


FIGURE 1 | State of the field of technetium alkyne complexes [1–6, 33, 34].

during the past decades and indeed some reaction products requiring the intermediary coordination of an alkyne (followed by the immediate isomerization to a vinylidene carbene) but also an insertion product with a technetium hydride could be isolated [1–6, 39]. Besides a fundamental interest, side-on bonded alkyne ligands increase the number of donor atoms per formal vacant coordination site at the metal, which, if installed into the scaffold of a polydentate chelator, could lead to a significant stabilization of the resulting chelate complexes. Both organotechnetium and chelate complexes separately represent invaluable workhorses in radiopharmaceutical imaging using the short-lived  $\gamma$ -emitting nuclear technetium isomer  $^{99m}\text{Tc}$  (e.g.,  $^{99m}\text{Tc}$ -sestamibi or  $^{99m}\text{Tc}$ -MAG3) [40, 41]. Also, other organotechnetium complexes such as those containing, e.g.,  $\{\text{Tc}^{\text{I}}(\text{CO})_3\}^+$  or Tc-coordinating cyclopentadienyl ligands are recent, robust and versatile additions to the tool box of nuclear medicinal researchers [42–71]. The introduction of extra donor atoms to a potential alkyne ligand may also favor the coordination of the alkyne moiety kinetically. Tolane-based pincer ligands containing a central alkyne unit were reported to form complexes with the desired coordination mode for a number of elements in the periodic table (Figure 2; compiled in S5.2–S5.4) [72–85].

To prevent a very common, and not yet fully understood [86], cyclization side-reaction of such potential ligands, a fluorinated, arsenic-based ligand was recently developed [84, 85]. The choice of the ligand substitution pattern for this study was a compromise of reactivity, stability, and solubility. Tentatively, As was chosen over P as the P derivatives are more electron-rich and therefore more prone to cyclization. Similarly, the  $\text{CF}_3$  groups deplete the ligands electron density further, reducing the tendency for cyclization to pentalenes and stabilizing the ligands against oxidation of the ligand backbone, while simultaneously increasing the solubility of formed complexes. While  $^t\text{Bu}$  substituents at the pnictogen atom usually stabilize the formed complexes by steric shielding of the metal, they hinder the kinetic introduction of

the ligand and destabilize the ligand framework (at least for P derivatives) for cyclization. Hence,  $^t\text{Bu}$  and  $^i\text{Pr}$  As,CC,As ligands with  $\text{CF}_3$ -substitution at the flanks were chosen as the tentatively most promising candidates for the present work.

In this work, the first structurally authenticated complexes of technetium containing side-on bonded alkyne ligands — not only with the long-lived  $^{99}\text{Tc}$  but also with its medically relevant nuclear isomer  $^{99m}\text{Tc}$  — are reported. The coordinated alkyne is tethered by flanking dialkylarylsarsine groups in an As,CC,As pincer ligand, forcing a  $\pi$ -coordination of the alkyne to technetium.

## 2 | Results and Discussion

To understand whether the endeavor for technetium alkyne complexes is even theoretically feasible, preceding density functional theory (DFT) calculations on the B3LYP-D3/def2-QZVPP level with an implicit solvation model for tetrahydrofuran were performed for hypothetical zero valent  $[\text{M}^0 \cdots (\text{HC}\equiv\text{CH})]$  ( $\text{M} = 3\text{d}, 4\text{d}, 5\text{d}$  metal) model complexes with a side-on  $\pi$ -coordinating alkyne and their  $[\text{M}^0=\text{C}=\text{CH}_2]$  vinylidene isomers for all d-group elements (details are given as Supporting Information: S4.15). Both isomers were stable for technetium and rhenium and the bonding parameter trends for the group 7 elements fit well in between those observed for group 6 and group 8. Thus, it can be concluded that the experimentally observed, problematic isomerization of side-on coordination of alkynes to vinylidene carbenes is not intrinsic but rather subject to influences of the accompanying ligand sphere around the metal. This was computationally confirmed by calculations on the B3LYP-D3/def2-QZVPP level for isostructural model complexes of groups 6, 7, and 8 with a  $[\text{MNC}_2(\text{AsH}_3)_2(\text{C}_2\text{H}_2)]^{+/0/-}$  ( $\text{M} = \text{Cr}, \text{Mo}, \text{W}, \text{Mn}, \text{Tc}, \text{Re}, \text{Fe}, \text{Ru}, \text{Os}$ ) donor set (details are given as Supporting Information: S4.16). Although the nitrido complexes show a clear energetic preference

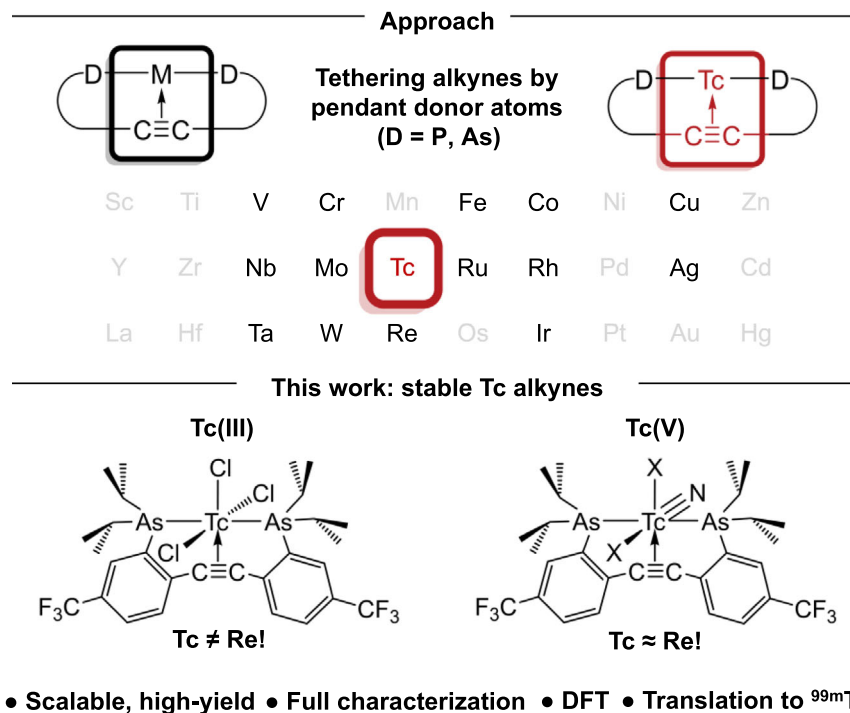


**FIGURE 2** | The approach used in this work based on previous literature precedent for  $D,CC,D$  ( $D = P, As$ ) complexes across the periodic table [72–85], and the scope of this work.

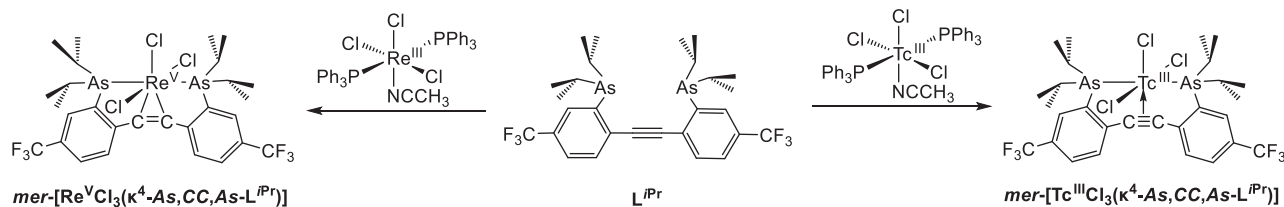
of the vinylidene structure, a reasonable chance for the existence of technetium alkyne complexes under the correct circumstances was deduced as the differences were relatively small in the order of ca. 20 kJ/mol. The group 7 elements Mn, Tc, and Re feature stable complexes in over seven different oxidation states. Given that alkyne complexes can draw significant stabilization from backdonation of electron rich metal centers [87, 88], and that low-valent rhenium alkynes appear to be somewhat more readily available [7, 8], low-valent alkyne complexes were focused initially. First, experiments with a sterically encumbered and normally more robust *tert*-butyl substituted potential *As,CC,As* ligand and  $[Tc^{III}Cl_3(PPh_3)_2(NCCH_3)]$  led to cyclization of the arsine-substituted alkyne as verified by x-ray diffraction (see S2.8, S5.9) and intractable decomposition of the technetium starting material. Such reactions are frequently observed and often complex involving multi-step ionic and radical pathways, thus, further analysis is beyond the scope of the present communication [86].

## 2.1 | Technetium(III) Alkyne Complex

The fluorinated, *iso*-propyl substituted ligand  $L^{iPr}$  instead reacted with both, the technetium(III) and rhenium(III) starting materials,  $[Tc^{III}Cl_3(PPh_3)_2(NCCH_3)]$  and  $[Re^{III}Cl_3(PPh_3)_2(NCCH_3)]$  giving the desired products  $[MCl_3(\kappa^4-As,CC,As-L^{iPr})]$  (Scheme 1).

While the ligand exchange reactions with  $L^{iPr}$  are robust and not directly sensitive to ambient oxygen or water, inadvertent oxidation of the released  $PPh_3$  must be avoided for isolation of the target products in high yield and purity due to co-crystallization of  $OPPh_3$  (crystal quality consistently low; see S2.4, S5.5). The rhenium-containing product was isolated as a dia-

magnetic green–gray powder, while the technetium-containing product was isolated as paramagnetic deep red microcrystals ( $\mu_{eff}(CD_2Cl_2) \approx 2.3$ ). As expected for the octahedral  $d^4$  system containing Tc(III), the  $^1H$  NMR spectrum of this product is not instructive. The  $^{19}F\{^1H\}$  NMR spectrum on the other hand shows only a single, narrow resonance for the  $CF_3$  groups at ca. –20 ppm being indicative of a symmetric ligand arrangement, however, ambiguity remains due to the clear influence of electron spin density in proximity to the  $CF_3$  groups. In contrast, a symmetric arrangement of the ligand in the diamagnetic rhenium complex can be concluded unambiguously from the observation of two sets of NMR resonances for the methyl groups of the *iso*-propyl substituents (*syn/anti* to the aromatic ring). The  $^{13}C$  NMR resonance of the alkyne carbon atoms in the rhenium complex are shifted by almost 90–174 ppm from 95 ppm observed for the same carbon atoms in the free ligand [85], suggesting a considerable contribution of a rhenacyclopropene resonance structure [72, 73, 77, 89–93]. Consistent with the spectroscopic properties, the rhenium complex could tentatively be formulated as *mer*- $[Re^VCl_3(\kappa^4-As,CC,As-L^{iPr})]$  with a dianionic  $4e^-$  donor alkyne unit and a  $d^2$  metal ion. Contrastingly for technetium, a classical side-on alkyne complex, *mer*- $[Tc^{III}Cl_3(\kappa^4-As,CC,As-L^{iPr})]$ , with the alkyne acting as a  $2e^- \pi$ -donor was derived. A similar electronic situation had been observed for non-fluorinated  $D,CC,D$  ( $D = P, As$ ) rhenium complexes before [73]. However, this remarkable difference in electronic structure between the isostructural complexes of technetium and rhenium warranted a more in-depth analysis and, hence, dark red single crystals of the technetium compound as well as dark green single crystals of the rhenium complex were grown by slow evaporation of  $CH_2Cl_2$  solutions and analyzed by x-ray diffraction. The solid-state structures of both products are shown in Figure 3.



**SCHEME 1** | Reaction of  $L^{iPr}$  with isostructural starting materials  $[M^{III}Cl_3(PPh_3)_2(NCCH_3)]$  ( $M = Tc, Re$ ).

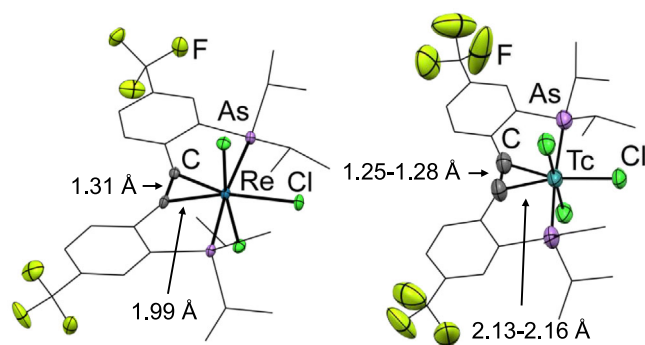


**FIGURE 3** | Molecular structures of the alkyne complexes  $mer-[Re^V Cl_3(\kappa^4-As, CC, As-L^{iPr})]$  and  $mer-[Tc^{III} Cl_3(\kappa^4-As, CC, As-L^{iPr})]$  (bond parameters compiled in Table 1). Ellipsoids are shown at 50% probability. Hydrogen atoms, disorder of the freely rotating  $CF_3$  groups and further labels are omitted for clarity. Skeletal carbon atoms are shown as wireframe for clarity.

The significant elongation of the  $C\equiv C$  bond and contraction of the alkyne distance to rhenium (1.31 Å, 1.88 Å) in  $mer-[Re^V Cl_3(\kappa^4-As, CC, As-L^{iPr})]$  compared to the contracted  $C\equiv C$  bond and elongation of the alkyne distance to technetium (< 1.25 Å, > 2.00 Å) in  $mer-[Tc^{III} Cl_3(\kappa^4-As, CC, As-L^{iPr})]$  is a clear indicator of the different bonding situations in the structurally similar complexes. In line with this interpretation, the  $Ar-C\equiv C$  angles are smaller for the rhenium compound compared to its technetium counterpart. DFT calculations on the B3LYP-D3/def2-TZVP ( $d^2$ : s,  $d^4$ -ls: t,  $d^4$ -hs: quint) revealed a low energy singlet  $Re^V$  ( $d^2$ ) configuration ( $d^4$ -ls: +3 kJ/mol,  $d^4$ -hs: +222 kJ/mol) consistent with the diamagnetism of the isolated complex matching the experimental geometry (exp.:  $Re-C \approx 2.00$  Å; calc.:  $d^2 \approx 2.00$  Å;  $d^4$ -ls  $\approx 2.13$  Å;  $d^4$ -hs  $\approx 2.16$  Å). Contrastingly and in accordance with the experimental observations, a paramagnetic  $d^4$ -ls ( $Tc^{III}$ ) configuration with two unpaired electrons is energetically preferred for technetium ( $d^2$ : +24 kJ/mol,  $d^4$ -hs: +222 kJ/mol) and consistent with the observed x-ray structure (exp.:  $Tc-C \approx 2.15$  Å; calc.:  $d^2 \approx 2.00$  Å;  $d^4$ -ls  $\approx 2.15$  Å;  $d^4$ -hs  $\approx 2.20$  Å). In the hypothetical (see S5.7)  $MnCl_3$  analogs, the  $d^4$ -hs configuration featuring an uncoordinated  $C\equiv C$  was most stable ( $d^2$ : +245 kJ/mol;  $d^4$ -ls: +96 kJ/mol; details are provided as Supporting Information: S4.1) suggesting that the metallacyclopropene resonance structure contributes less when moving up the group 7 elements due to gradually increased spin-pairing when moving down the group. Previously reported topological analyses of experimentally determined electron densities of  $2e^-$  and  $4e^-$  alkynes proved that a convex distortion of the bond paths is observed for  $4e^-$  alkyne donors, while a concave shape is characteristic of  $2e^-$  alkyne ligands [93]. An analogous topological

**TABLE 1** | Selected bond lengths and angles in the  $\{MCl_3\}$ -containing complexes of  $L^{iPr}$ . The second set of parameters for  $mer-[Tc^{III} Cl_3(\kappa^4-As, CC, As-L^{iPr})] \cdot 0.5CH_2Cl_2$  are those of a second independent molecule in the asymmetric unit.

Bond lengths [Å]	$mer-[Re^V Cl_3(\kappa^4-As, CC, As-L^{iPr})]$	$mer-[Tc^{III} Cl_3(\kappa^4-As, CC, As-L^{iPr})] \cdot 0.5CH_2Cl_2$
$C\equiv C$	1.309(4)	1.25(2) 1.28(2)
$M-C_{\equiv C}$	1.986(2) 1.994(3)	2.13(1) 2.13(1) 2.13(1) 2.16(1)
$M \cdots \text{centroid}(C\equiv C)$	1.879	2.037 2.048
$M-Cl_{\text{trans}-C\equiv C}$	2.4399(7)	2.423(3) 2.433(3)
$M-Cl_{\text{trans}-Cl}$	2.3878(7) 2.3884(8)	2.343(4) 2.338(3) 2.365(4) 2.358(3)
$M-As$	2.5512(7) 2.5515(7)	2.572(1) 2.564(1) 2.572(1) 2.565(2)
Angles [°]		
As-	93.8	92.4 92.5
$M \cdots \text{centroid}(C\equiv C)$	93.8	92.8 93.2
Cl-	94.7	89.1 89.0
$M \cdots \text{centroid}(C\equiv C)$	94.9	89.4 89.2
	179.1	179.3 178.8
$Ar-C(\equiv CR)-M$	136.4(2) 136.7(2)	129.7(9) 128.8(8) 131.1(9) 130.2(8)
$Ar-C\equiv C$	152.3(3) 152.8(3)	155(1) 156(1) 158(1) 159(1)
As-M-As	172.37(2)	174.61(9) 172.79(5)
Cl-M-Cl	84.49(3) 85.94(3) 170.42(3)	90.0(1) 89.6(1) 91.6(1) 92.1(1) 177.3(1) 177.8(1)

analysis of the calculated electron density  $\rho(r)$  in the present case revealed a concave shape of the bond paths connecting the  $Tc-C$  (3,-1) critical points ("bond") with the (3,-3) critical points (atomic positions) for the most stable electron configuration of  $mer-[Tc^{III} Cl_3(\kappa^4-As, CC, As-L^{iPr})]$ , consistent with the presumed  $2e^-$  donor mode of the central alkyne unit (details S4.1). Contrastingly and characteristic for the presumed  $4e^-$  donor situation, convex bond paths are obtained for the  $\{ReCl_3\}$  analog. The topological features are depicted on electron localization function (ELF) mappings in the  $M \cdots C-C$  plane in Figure 4 (complementary plots: S4.2–S4.14).

To better understand the d orbital splitting in both Tc and Re compounds, the geometry around the rhenium ion in the

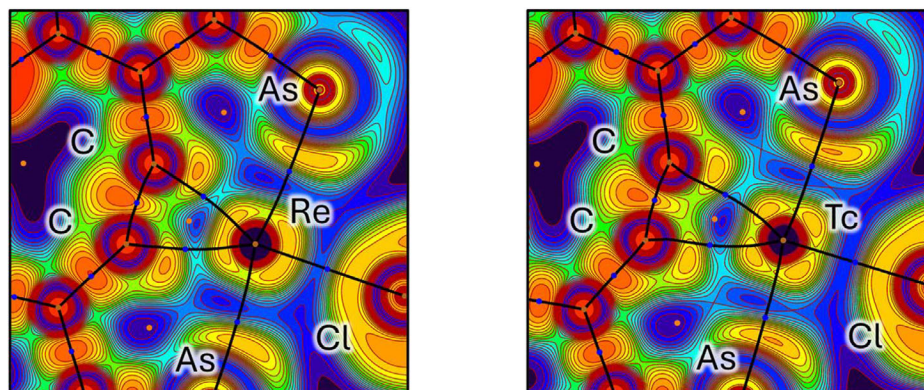


**FIGURE 4** | DFT-based Electron localization function (ELF) maps of  $mer\text{-}[\text{Re}^{\text{V}}\text{Cl}_3(\kappa[4]\text{-As,CC,As-L}^{\text{iPr}})]$  and  $mer\text{-}[\text{Tc}^{\text{III}}\text{Cl}_3(\kappa[4]\text{-As,CC,As-L}^{\text{iPr}})]$  including topological features of the electron density (brown: (3,-3) critical points; blue: (3,-1) critical points; orange: (3,+1) critical points; black: bond paths connecting (3,-3) and (3,-1) critical points) of  $\rho(r)$  in the  $\text{M}\cdots\text{C}\equiv\text{C}$  plane.

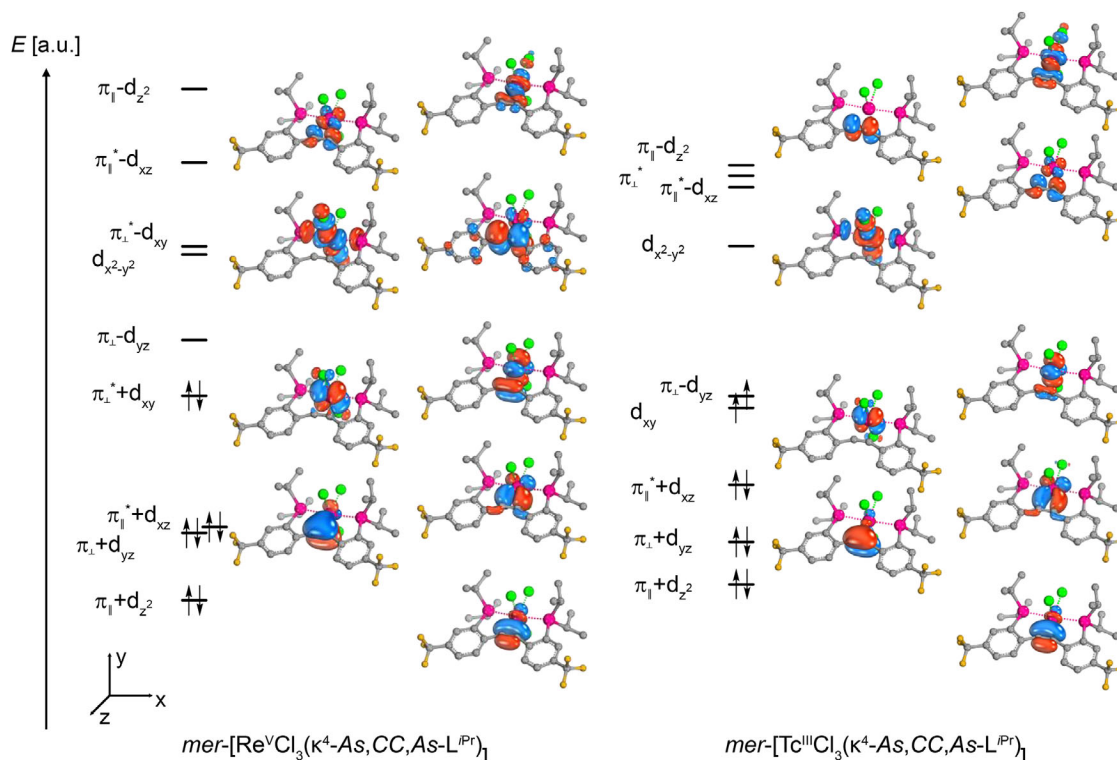
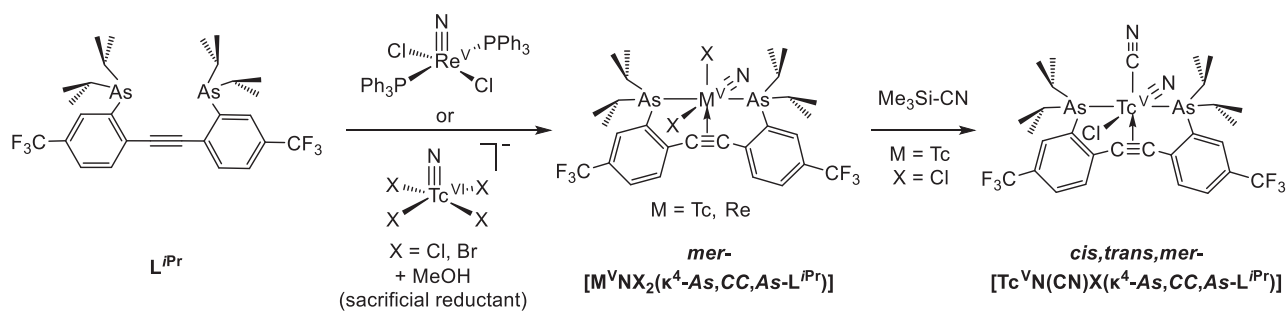


**FIGURE 5** | CAS(8,9) orbital interactions in  $mer\text{-}[\text{Re}^{\text{V}}\text{Cl}_3(\kappa^4\text{-As,CC,As-L}^{\text{iPr}})]$  (left) and  $mer\text{-}[\text{Tc}^{\text{III}}\text{Cl}_3(\kappa^4\text{-As,CC,As-L}^{\text{iPr}})]$  (right). The CAS is constructed from the alkyne  $\pi$  orbitals ( $\pi_{\parallel}$ ,  $\pi_{\perp}$ ,  $\pi_{\parallel}^*$ ,  $\pi_{\perp}^*$ ) and the five metal d orbitals respectively. Further ligand interactions were omitted.



**SCHEME 2** | Reaction of  $\text{L}^{\text{iPr}}$  with rhenium and technetium nitrido starting materials.

complex was assessed using the SHAPE algorithm (see Table S9) [94–97]. In both cases an octahedral geometry with a centroid(C≡C)+2As+3Cl donor set was a closer fit than all other potential hexacoordinate geometries with a shape measure of 0.65 (including idealized heptacoordinate geometries with a 2C+2As+3Cl donor set and a minimum shape measure of 4.95 for a pentagonal bipyramidal geometry). The formal d-orbital splitting of Re derived from an octahedral ligand field is, thus, qualitatively understood when thinking about the considerable bond length differences between the co-ligand donor atoms with the  $d_z^2$  orbital oriented in the M...centroid(C≡C) axis. As such, the lowest lying orbital of nearly pure d character should be oriented in direction of the As–M–As axis—lying in the  $xy$  plane. Natural bonding orbital (NBO) analyses using NBO6.0 confirm this interpretation and only a single Re-centered d-orbital,  $d_{xy}$ , can be localized for the singlet structure of  $mer$ -[Re<sup>V</sup>Cl<sub>3</sub>( $\kappa^4$ -As,CC,As-L<sup>iPr</sup>)], while one doubly filled and two singly filled orbitals with mainly metal-centered d orbital character can be identified for  $mer$ -[Tc<sup>III</sup>Cl<sub>3</sub>( $\kappa^4$ -As,CC,As-L<sup>iPr</sup>)]. Complete active space self-consistent field (CAS-SCF) multireference calculations are consistent with the energetic predictions of the DFT calculations providing the lowest energy for a singlet  $d^2$  electron configuration for Re and a triplet  $ls-d^4$  for Tc (details given in S4.1). The orbitals involved in the alkyne...M interaction according to the underlying d-orbital energy splitting can be evaluated from such calculations as depicted in Figure 5.

The suspected formal oxidation states of the central metal ions and the As, CC, As ligands were finally confirmed by localized orbital bonding analysis (LOBA) [98]. Although the assignment of oxidation states especially by theoretical methods is strictly formal and can be ambiguous [99, 100], the exhaustive body of evidence in the present case suggests that  $mer$ -[Re<sup>V</sup>Cl<sub>3</sub>( $\kappa^4$ -As,CC,As-L<sup>iPr</sup>)] is indeed best described as a formal Re<sup>V</sup> species with a dianionic 4e<sup>-</sup> alkyne donor, while a neutral pincer, 2e<sup>-</sup> donor ligand and Tc(III) are formulated for  $mer$ -[Tc<sup>III</sup>Cl<sub>3</sub>( $\kappa^4$ -As,CC,As-L<sup>iPr</sup>)]. The formation of a metallacyclopriene resonance structure through backdonation of the metals d electrons into alkyne  $\pi^*$  orbitals and contraction of the M–C bonds contributes significantly to the stabilization of low valent transition metal alkyne complexes. Therefore, the lack of this resonance structure can explain the difficulties that are frequently encountered during the attempted syntheses of low valent technetium alkyne complexes. Even with the tethered alkyne ligands of the present communication, reactions with common starting materials containing the metal in even lower oxidation states, that is, those with the *fac*-{Tc(CO)<sub>3</sub>}<sup>+</sup>, {Tc<sup>I</sup>(NO)}<sup>2+</sup> or {Tc<sup>II</sup>(NO)}<sup>3+</sup> cores, but also reactions with a slightly varied *tert*-butyl substituted ligand led to undesired side-reactions in our hands and no technetium-containing products were identified (for details see S2.9, S5.8).

## 2.2 | Technetium(V) Alkyne Complexes

Thus, complexes with technetium in a higher formal oxidation state that would favor the formation of classic 2e<sup>-</sup> alkyne complexes became naturally interesting and related reactions are compiled in Scheme 2.

A remarkable difference between rhenium and technetium was observed during the attempted synthesis of nitrido metal(V) complexes. While the nearly insoluble rhenium(V) complex *trans*-[Re<sup>V</sup>NCl<sub>2</sub>(PPh<sub>3</sub>)<sub>2</sub>] readily exchanges the two triphenylphosphine ligands for the pincer ligand forming *mer*-[Re<sup>V</sup>NCl<sub>2</sub>( $\kappa^4$ -As,CC,As-L<sup>iPr</sup>)] in good yields after some days, the technetium analog *trans*-[Tc<sup>V</sup>NCl<sub>2</sub>(PPh<sub>3</sub>)<sub>2</sub>] proved practically inert. Instead and as an established work-around for the inertness of *trans*-[Tc<sup>V</sup>NCl<sub>2</sub>(PPh<sub>3</sub>)<sub>2</sub>] in technetium chemistry, a reaction with [Tc<sup>VI</sup>NX<sub>4</sub>]<sup>-</sup> (X = Cl, Br) using methanol as a sacrificial reductant readily led to the formation of *mer*-[Tc<sup>V</sup>NX<sub>2</sub>( $\kappa^4$ -As,CC,As-L<sup>iPr</sup>)] in excellent yields. The <sup>13</sup>C NMR resonances of the alkyne carbon atoms in *mer*-[Tc<sup>V</sup>NX<sub>2</sub>( $\kappa^4$ -As,CC,As-L<sup>iPr</sup>)] are observed around 110 ppm, while those of *mer*-[Re<sup>V</sup>NCl<sub>2</sub>( $\kappa^4$ -As,CC,As-L<sup>iPr</sup>)] are found around 120 ppm, both of which are consistent with a formulation as side-on bonded alkyne complexes acting as classic 2e<sup>-</sup> donor ligands when comparing it to the <sup>13</sup>C NMR resonance observed for the same atoms in the free ligand L<sup>iPr</sup> (95 ppm). DFT calculations on the B3LYP-D3/def2-TZVP level confirm the assignment as classic 2e<sup>-</sup> donor alkyne units based on topological descriptors. The <sup>1</sup>H NMR spectra of the nitrido complexes show a characteristic set of four resonances reflecting each potential orientation of the methyl groups in the *iso*-propyl substituents of the complexes (*syn/anti* to M≡N, *syn/anti* to the aromatic ring) as well as two resonances for the tertiary C–H protons (*syn/anti* to M≡N) verifying the expectedly lower molecular symmetry compared to the trichloro complexes described above. The oxidation states of the products are readily verified by their characteristic  $\nu$ (Tc≡N) around 1040 cm<sup>-1</sup>, which is in the common range for Tc(V) nitrido complexes and somewhat red-shifted compared to the analogous  $\nu$ (Re≡N) 1054 cm<sup>-1</sup>. No appreciable decomposition was observed even when heating for hours at 100°C in air. The reactivity and derivatization potential of the nitrido complexes as platforms for systematic studies on the technetium-alkyne bonds or for potential labeling with biologically relevant molecules by ligand exchange procedures was probed by reactions using silver or silyl-based halide scavengers and bidentate ligands like bipyridine or *N,N*-dialkylbenzoylthiourea derivatives. The alkyne complexes generally appear to be inert toward bidentate ligands and the starting material was recovered unchanged even after prolonged heating in boiling toluene. The more aggressive derivatization agent Me<sub>3</sub>Si–CN cleanly reacted with *mer*-[Tc<sup>V</sup>NCl<sub>2</sub>( $\kappa^4$ -As,CC,As-L<sup>iPr</sup>)] forming a single, well-defined product in near quantitative isolated yield: *cis,trans,mer*-[Tc<sup>V</sup>N(CN)Cl( $\kappa^4$ -As,CC,As-L<sup>iPr</sup>)], while preliminary reactions with other silyl reagents were so far less successful (i.e., no reaction between *mer*-[Tc<sup>V</sup>NBr<sub>2</sub>( $\kappa^4$ -As,CC,As-L<sup>iPr</sup>)] and Me<sub>3</sub>Si–N<sub>3</sub> and decomposition during the crystallization of the initial product formed from the reaction between *mer*-[Tc<sup>V</sup>NCl<sub>2</sub>( $\kappa^4$ -As,CC,As-L<sup>iPr</sup>)] and Me<sub>3</sub>Si–NCS; for further details see: S2.7, S5.10). The product is readily identified as a mono cyanido complex by the presence of a single C≡N stretching frequency at 2139 cm<sup>-1</sup> in the infrared spectrum, while the stereochemical *trans*-arrangement of the cyanido ligand to the alkyne can be inferred from the blue-shift of  $\nu$ (RC≡CR) to 1956 cm<sup>-1</sup> whereas  $\nu$ (Tc≡N) remains essentially unchanged at 1038 cm<sup>-1</sup> compared to the starting material. Even prolonged heating using an excess of Me<sub>3</sub>Si–CN did not lead to a second ligand exchange reaction or decomposition. X-ray quality crystals of the product were obtained directly from the reaction mixture confirming the spectroscopic assignment as a mono cyanido complex. The other

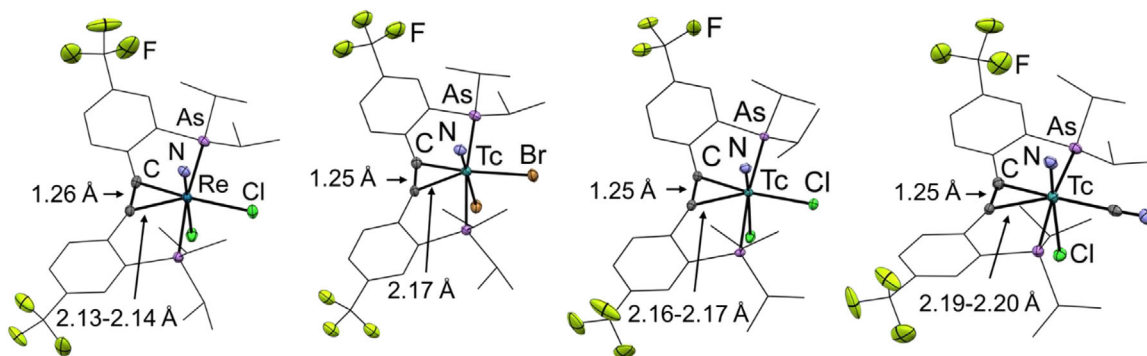


**FIGURE 6** | Molecular structures of the alkyne complexes  $mer\text{-}[M^V NCl_2(\kappa^4\text{-As,CC,As-L}^{iPr})]$  ( $M = \text{Tc, Re}$ ),  $mer\text{-}[Tc^V NBr_2(\kappa^4\text{-As,CC,As-L}^{iPr})]$  and  $cis,trans,mer\text{-}[Tc^V N(CN)Cl(\kappa^4\text{-As,CC,As-L}^{iPr})]$ . Ellipsoids are shown at 50% probability. Hydrogen atoms, disorder of the freely rotating  $CF_3$  groups and further labels are omitted for clarity. Skeletal carbon atoms are shown as wireframe for clarity. The bond parameters are compared in Table 2.

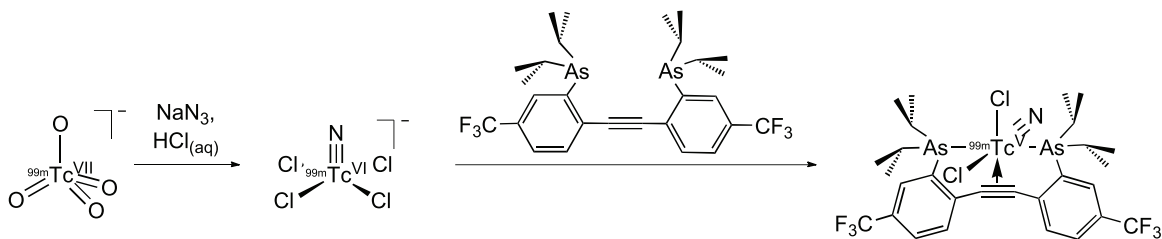
**TABLE 2** | Selected bond lengths and angles in the rhenium and technetium nitrido alkyne complexes.

Bond lengths [Å]	$mer\text{-}[Re^V NCl_2(\kappa^4\text{-As,CC,As-L}^{iPr})]$	$mer\text{-}[Tc^V NBr_2(\kappa^4\text{-As,CC,As-L}^{iPr})]$	$mer\text{-}[Tc^V NCl_2(\kappa^4\text{-As,CC,As-L}^{iPr})]$	$cis,trans,mer\text{-}[Tc^V N(CN)Cl(\kappa^4\text{-As,CC,As-L}^{iPr})]$
$C\equiv C$	1.262(4)	1.250(6)	1.254(3)	1.248(6)
$M\text{-}C_{C\equiv C}$	2.129(3) 2.137(3)	2.165(4) 2.167(4)	2.161(2) 2.165(2)	2.193(4) 2.195(4)
$M\cdots\text{centroid}(C\equiv C)$	2.038	2.074	2.070	2.103
$M\equiv N$	1.671(2)	1.634(3)	1.630(2)	1.680(1)
$M\text{-}X_{\text{trans-}C\equiv C}$	2.4191(8)	2.5661(7)	2.4207(7)	2.151(4)
$M\text{-}X_{\text{trans-M}\equiv N}$	2.6980(8)	2.9003(7)	2.7262(7)	2.680(1)
$M\text{-As}$	2.5490(5) 2.5541(5)	2.5423(6) 2.5504(6)	2.5402(5) 2.5464(5)	2.5439(6) 2.5442(6)
$C\equiv N$	—	—	—	1.103(6)
Angles [°]				
$N\equiv M\cdots\text{centroid}(C\equiv C)$	99.6	100.1	99.4	99.9
$As\text{-}M\cdots\text{centroid}(C\equiv C)$	92.5 93.1	92.3 92.8	92.2 92.9	92.4 92.6
$X\text{-}M\cdots\text{centroid}(C\equiv C)$	79.8 162.0	78.6 162.0	78.8 162.1	82.6 163.7
$Ar\text{-}C(\equiv CR)\text{-}M$	130.7(2) 131.1(2)	129.1(3) 129.6(3)	129.2(2) 129.7(2)	128.0(3) 128.1(3)
$Ar\text{-}C\equiv C$	156.2(3) 156.4(3)	157.3(4) 157.6(4)	157.4(2) 157.4(2)	157.9(4) 158.4(4)
$N\equiv M\text{-}X$	98.43(9) 176.08(9)	97.8(1) 177.5(1)	98.54(7) 175.45(7)	86.1(1) 177.4(1)
$N\equiv M\text{-As}$	92.07(9) 92.22(9)	93.0(1) 93.2(2)	92.32(7) 92.48(7)	91.8(1) 92.7(1)
$As\text{-}M\text{-As}$	172.35(2)	171.19(2)	172.36(2)	172.62(2)
$X\text{-}M\text{-}X$	82.35(2)	83.53(2)	83.40(2)	82.9(1)

technetium nitrido complexes also crystallized from the reaction mixture as large, colorless blocks that were suitable for x-ray diffraction (solid-state structures shown in Figure 6, selected bonding parameters are compared in Table 2).

### 2.3 | $^{99m}\text{Tc}$ Alkyne Complex

The presented technetium alkyne complexes can be isolated under ambient conditions and they are relatively inert toward



**SCHEME 3** | Preparation of  $mer\text{-}[^{99m}\text{Tc}^{\text{V}}\text{NCl}_2(\kappa^4\text{-As,CC,As-L}^{\text{iPr}})]$ .

competing ligands. They are therefore sufficiently robust under conditions that are feasible for potential radiopharmaceutical applications and the synthesis of  $^{99m}\text{Tc}$  complexes became interesting. While the arsenic-based complexes of the present study are obviously not directly suitable for such applications due to the toxicity and high lipophilicity of organoarsenic compounds, the translation to  $^{99m}\text{Tc}$  proves the viability of the initial hypothesis that the integration of alkyne donors into chelator frameworks can result in exceedingly stable donor sets for the tethering biomolecules to the radiometal. Metal-tethering of small peptides by pendant alkyne donors has been achieved, e.g., for tungsten before. [101] In a proof of concept, a synthetic protocol akin to the procedure for the  $^{99}\text{Tc}$  compound described above was derived via  $[\text{}^{99m}\text{Tc}^{\text{VI}}\text{NCl}_4]^-$  to provide  $mer\text{-}[^{99m}\text{Tc}^{\text{V}}\text{NCl}_2(\kappa^4\text{-As,CC,As-L}^{\text{iPr}})]$  (Scheme 3).

It is well-known that protocols for the preparation of the  $^{99m}\text{Tc}$  nitrido precursor frequently lead to complex mixtures of variable composition [102]. This is not a serious issue as the final products can commonly be purified easily from traces of the inadvertently formed left-over side-products by standard solid state extraction following immobilization on a reverse phase chromatographic column after chelation [102]. This holds true in the present reaction, where inadvertent side-products from the starting material synthesis were readily removed by chromatographic purification. Once formed, the chelate complex remained stable as verified by repeated, decay-corrected HPLC analysis of the purified complex  $mer\text{-}[^{99m}\text{Tc}^{\text{V}}\text{NCl}_2(\kappa^4\text{-As,CC,As-L}^{\text{iPr}})]$ . The HPLC trace did not show significant decomposition during the decay time of  $^{99m}\text{Tc}$  suggesting alkyne-units as suitable donor building blocks for the generation of stable technetium chelate complexes for medicinal applications.

### 3 | Conclusion

Alkyne complexes of technetium — a compound class that had eluded isolation attempts for decades with technetium being the last d-block element in periods 4, 5, and 6 without known side-on alkyne ligands — have finally been isolated by forcing the side-on coordination of an internal  $\text{C}\equiv\text{C}$  triple bond using an  $\text{As,CC,As}$  tolane-based pincer ligand. Technetium alkyne complexes have a lower tendency to form  $4e^-$  metallacyclopropene resonance structures in comparison to their isostructural heavier homolog rhenium. The electronic differences have consequences for the reactivity of the technetium compounds, especially when compared with their rhenium congeners and are at least in part responsible for the difficulties encountered in previous preparation attempts. The alkyne motif was proven to coordinate the medically relevant nuclear isomer  $^{99m}\text{Tc}$  at the tracer level

under formation of stable chelates that structurally resemble their  $^{99}\text{Tc}$  and  $\text{Re}$  analogs. Thus,  $\text{C}\equiv\text{C}$  triple bonds are suggested as valuable design motifs for future radiopharmaceutical chelators providing excellent stability for tethering of technetium to biologically active molecules.

#### Author Contributions

**Maximilian Roca Jungfer:** conceptualization, methodology, investigation, validation, funding acquisition, visualization, writing – original draft, writing – review and editing, project administration, resources, supervision, data curation, formal analysis, software. **Moritz Johannes Ernst:** formal analysis, investigation, methodology, writing - review & editing, translation. **Lukas Eberle:** formal analysis, investigation, methodology, writing - review & editing. **Marius Kesselring:** investigation. **Guilhem Claude:** formal analysis, investigation, resources, writing - review & editing. **Joachim Ballmann:** funding acquisition, investigation, resources.

#### Acknowledgements

The authors thank Prof. Dr. Nina Huittinen for hosting MRJ as a scientific guest researcher and allowing the work on technetium to be completed in the radiochemical laboratories at Freie Universität Berlin. The authors thank Prof. Dr. Ulrich Abram for providing the technetium used in the preparative work. The authors thank Prof. Dr. Christian Müller (Freie Universität Berlin) for measurement time and for supporting MJE to contribute to this work. The authors thank Jacqueline Grewe and Dr. Mathias Ellwanger for their support with regard to radiation protection and laboratory organization. LE thanks Prof. Dr. L. H. Gade for generous support. The authors thank Karlsruhe Institute of Technology (KIT), Freie Universität Berlin and Universität Heidelberg for resources. The authors acknowledge support by the KIT Publication Fund of the Karlsruhe Institute of Technology enabling Open Access publishing. The contributions of Joachim Ballmann to this work are acknowledged *post mortem*. As a friend, mentor and colleague his kind-hearted nature, vigor and passion for science continue to inspire our quest for excellence.

Open access funding enabled and organized by Projekt DEAL.

#### Funding

Fonds der Chemischen Industrie (FCI), Liebig fellowship to MRI. The state of Baden-Württemberg through bwHPC (JUSTUS cluster). German Research Foundation grant INST 40/467-1 FUGG (JUSTUS cluster) and BA 4859/3-2 (LE, JB). Open Access enabled by Karlsruhe Institute of Technology KIT Publication Fund (Project DEAL).

#### Conflicts of Interest

The authors declare no conflicts of interest.

## Data Availability Statement

The data that supports the findings of this study are available in the supplementary material of this article. Original data (e.g., spectra files) are available from the corresponding author upon reasonable request.

## References

1. M. Roca Jungfer and M. L. Besmer, "Structural Organometallic Chemistry of Technetium," *Advances in Organometallic Chemistry* 81 (2024): 271–328.
2. A. K. Burrell, J. C. Bryan, and G. J. Kubas, "Technetium–carbon Multiple Bonds: Synthesis and Structure of  $\text{Tc}(=\text{C}=\text{CHPh})\text{Cl}(\text{dppe})_2$  and  $[\text{Tc}(=\text{C}-\text{CH}_2-\text{tBu})\text{Cl}(\text{dppe})_2]^+$ ," *Organometallics* 13 (1994): 1067–1069, <https://doi.org/10.1021/om00016a007>.
3. A. Abdulkader, A. Hagenbach, and U. Abram, " $\text{Tc}(\text{NO})\text{Cl}(\text{Cp})(\text{PPh}_3)$ —A Technetium(I) Compound With an Unexpected Synthetic Potential," *European Journal of Inorganic Chemistry* 2021 (2021): 3812–3818, <https://doi.org/10.1002/ejic.202100521>.
4. M. Roca Jungfer and U. Abram, "Unlocking Air and Waterstable Technetium Acetylides and Other Organometallic Complexes," *Inorganic Chemistry* 61 (2022): 7765–7779, <https://doi.org/10.1021/acs.inorgchem.2c00070>.
5. M. J. Ernst, M. Roca Jungfer, and U. Abram, "Reactions of  $\text{Tc}^{\text{I}}(\text{NO})$  and  $\text{Tc}^{\text{V}}\text{N}$  Complexes With Alkynes and Alkynides," *Organometallics* 41 (2022): 2011–2021, <https://doi.org/10.1021/acs.organomet.2c00192>.
6. M. L. Besmer, H. Braband, T. Fox, B. Spingler, A. P. Sattelberger, and R. Alberto, "Binding Small Molecules to a Cis-dicarbonyl  $^{99}\text{Tc}^{\text{I}}$ -PNP Complex via Metal–ligand Cooperativity," *Inorganic Chemistry* 62 (2023): 10727–10735, <https://doi.org/10.1021/acs.inorgchem.3c01177>.
7. J. K. Felixberger, J. G. Kuchler, E. Herdtweck, R. A. Paciello, and W. A. Herrmann, "Alkyne Coordination to Organorhenium Oxides With Rhenium in High Oxidation States," *Angewandte Chemie International Edition* 27 (1988): 946–948, <https://doi.org/10.1002/anie.198809461>.
8. W. A. Herrmann, R. A. Fischer, and E. Herdtweck, "Alkyne Complexes of Rhenium in Intermediate Oxidation States: Synthesis and Molecular Structure of a Rhenium(V) Allenylidene Complex," *Angewandte Chemie International Edition* 26 (1987): 1263–1265, <https://doi.org/10.1002/anie.198712631>.
9. J. J. Kowalczyk, A. M. Arif, and J. A. Gladysz, "Synthesis, Structure, and Reactivity of Chiral Rhenium Alkyne Complexes of the Formula  $[(\eta^5\text{C}_5\text{H}_5)\text{Re}(\text{NO})(\text{PPh}_3)(\text{RC}\equiv\text{CR}')]^+\text{BF}_4^-$ ," *Organometallics* 10 (1991): 1079–1088, <https://doi.org/10.1021/om00050a045>.
10. A. M. Santos, C. C. Romão, and F. E. Kühn, " $(\eta^2\text{Alkyne})\text{methyl}(\text{dioxo})\text{Rhenium}$  Complexes as Aldehydeolefination Catalysts," *Journal of the American Chemical Society* 125 (2003): 2414–2415, <https://doi.org/10.1021/ja021315c>.
11. K. G. Caulton, "Coordination Chemistry of the Manganese and Rhenium Fragments  $(\text{C}_5\text{H}_5)\text{M}(\text{CO})_2$ ," *Coordination Chemistry Reviews* 38 (1981): 1–43, [https://doi.org/10.1016/S0010-8545\(00\)80498-1](https://doi.org/10.1016/S0010-8545(00)80498-1).
12. J. M. Mayer, T. H. Tulip, J. C. Calabrese, and E. Valencia, "Associative Ligand Substitution Reactions of Lowvalent Rheniumoxo Compounds: Crystal and Molecular Structures of  $[\text{ReO}(\text{MeC}\equiv\text{CMe})_2\text{L}]\text{SbF}_6$  (L = pyridine, 4,4'-dimethyl-2,2'-bipyridine)," *Journal of the American Chemical Society* 109 (1987): 157–163, <https://doi.org/10.1021/ja00235a024>.
13. J. K. Bera, P. E. Fanwick, and R. A. Walton, "Decarboxylation Reactions of Alkyne-carboxylic Acids as a Route to Multiply Bonded  $[\text{Re}_2]^{n+}$   $\mu$ -alkyne and  $\mu$ carbyne Complexes," *Dalton Transactions* 2001 (2001): 109–110, <https://doi.org/10.1039/b008265l>.
14. R. D. Adams, P. Dhull, M. Kaushal, and M. D. Smith, "The Activation and Transformations of Vinyl Acetate at a Dirhenium Carbonyl Center," *Journal of Organometallic Chemistry* 902 (2019): 120969, <https://doi.org/10.1016/j.jorganchem.2019.120969>.
15. D. M. Hoffman, J. C. Huffman, D. Lappas, and D. A. Wierda, "Alkyne Reactions With Rhenium(V) Oxo Alkyl Phosphine Complexes—Phosphine Displacement Versus Apparent Re–P Insertion," *Organometallics* 12 (1993): 4312–4320, <https://doi.org/10.1021/om00035a016>.
16. M. Ganesan, K. Y. Shih, P. E. Fanwick, and R. A. Walton, "Complexation of the Triply Bonded Dirhenium(II) Complex  $\text{Re}_2\text{Cl}_4(\mu\text{dppm})_2$  ( $\text{dppm} = \text{Ph}_2\text{PCH}_2\text{PPh}_2$ ) by up to Three Acetylene Molecules," *Inorganic Chemistry* 42 (2003): 1241–1247, <https://doi.org/10.1021/ic020532b>.
17. E. Spaltenstein, T. K. G. Erikson, S. C. Critchlow, and J. M. Mayer, "Low-valent Rheniumoxo Alkyl and Oxo Hydride Complexes: The Stabilizing Influence of the Oxo Ligand," *Journal of the American Chemical Society* 111 (1989): 617–623, <https://doi.org/10.1021/ja00184a032>.
18. D. S. Williams and R. R. Schrock, "Synthesis and Reactivity of a Series of Analogous Rhenium Tris(imido), Bis(imido) Alkyne, and Imido Bis(alkyne) Complexes," *Organometallics* 12 (1993): 1148–1160, <https://doi.org/10.1021/om00028a032>.
19. T. R. Cundari, R. R. Conry, E. Spaltenstein, et al., "Rheniumoxo-bis(acetylene) Anions: Structure, Properties, and Electronic Structure. Comparison of Re–O Bonding With That in Other Rheniumoxo Complexes," *Organometallics* 13 (1994): 322–331, <https://doi.org/10.1021/om00013a047>.
20. S. K. Tahmassebi, W. S. McNeil, and J. M. Mayer, "Hydroxide-, Amide-, and Sulfhydrylrhenium(I) Tris(alkyne) Complexes: Rearrangements to Rhenium(III) Bis(alkyne) Oxo and Nitrido Compounds," *Organometallics* 16 (1997): 5342–5353, <https://doi.org/10.1021/om9704814>.
21. Y. Han, C. J. Harlan, P. Stoessel, et al., "Rhenium Oxo Complexes of a Chelating Diyne Ligand: Synthesis and Study of the Kinetics of Protonation," *Inorganic Chemistry* 40 (2001): 2942–2952, <https://doi.org/10.1021/ic0100931>.
22. J. H. Jung, D. M. Hoffman, and T. R. Lee, "Synthesis, X-ray Crystallographic, and Reactivity Studies of Rhenium(V) Alkyne Complexes," *Journal of Organometallic Chemistry* 599 (2000): 112–122, [https://doi.org/10.1016/S0022-328X\(99\)00745-7](https://doi.org/10.1016/S0022-328X(99)00745-7).
23. H. W. Swidersky, O. Kindel, F. Weller, and K. Dehnicke, "Die Kristallstrukturen von  $[\text{ReCl}_4(\text{PhC}\equiv\text{CPh})_2]\cdot 2\text{CH}_2\text{Cl}_2$  und von  $\text{PPh}_4[\text{ReOCl}_4]$ ," *Zeitschrift für anorganische und allgemeine Chemie* 580 (1990): 18–26, <https://doi.org/10.1002/zaac.19905800103>.
24. T. Weidmann, V. Weinrich, B. Wagner, C. Robl, and W. Beck, "Dirhenioethin  $(\text{OC})_5\text{Re}-\text{C}\equiv\text{C}-\text{Re}(\text{CO})_5$  Als Baustein Zum Aufbau von Carbonyl-Metall-Clusterverbindungen," *Chemische Berichte* 124 (1991): 1363–1368, <https://doi.org/10.1002/cber.19911240609>.
25. S. Komiya and A. Baba, "Synthesis and Structure of Hydrido Bis(ethylene) and Hydrido Dinitrogen Complexes of Rhenium(I) Having Dimethylphenylphosphine Ligands," *Organometallics* 10 (1991): 3105–3110, <https://doi.org/10.1021/om00055a024>.
26. F. W. V. Einstein, K. G. Tyers, and D. Sutton, "Characterization of the Two-electron  $\eta^2$ -Alkyne Ligand in Cyclopentadienyldicarbonyl(alkyne)Rhenium Complexes. X-ray Structure of  $\text{Re}(\eta^5\text{C}_5\text{H}_5)(\eta^2\text{C}_2\text{Ph}_2)(\text{CO})_2$ ," *Organometallics* 4 (1985): 489–493, <https://doi.org/10.1021/om00122a010>.
27. R. R. Conry and J. M. Mayer, "Rhenium(I) Tris(acetylene) Complexes:  $\text{Re}(\text{OR})(\text{RC}\equiv\text{CR})_3$  and  $[\text{Re}(\text{L})(\text{RC}\equiv\text{CR})_3]\text{OTf}$ ," *Organometallics* 12 (1993): 3179–3186, <https://doi.org/10.1021/om00032a046>.
28. S. K. Tahmassebi and J. M. Mayer, "Synthesis and Reactivity of Rhenium(III) Sulfido Bis(acetylene) Iodide Complexes," *Organometallics* 14 (1995): 1039–1043, <https://doi.org/10.1021/om00002a059>.
29. B. Dudle, O. Blacque, and H. Berke, "Ethylene Reactions of a  $[\text{ReH}(\eta^2\text{BH}_4)(\text{NO})(\text{PPh}_3)_2]$  Complex: Reductive Elimination of Ethane and Oxidative Coupling to Butadiene," *Organometallics* 31 (2012): 1832–1839, <https://doi.org/10.1021/om201187w>.
30. E. Valencia, B. D. Santarsiero, S. J. Geib, A. L. Rheingold, and J. M. Mayer, "Synthesis and Characterization of Symmetrical and Unsymmetrical Lowvalent Rheniumoxo Dimers,  $\text{Re}_2\text{O}_2(\text{RC}\equiv\text{CR})_4$ ," *Journal of the American Chemical Society* 109 (1987): 6896–6898, <https://doi.org/10.1021/ja00256a078>.

31. C. P. Casey, T. E. Vos, J. T. Brady, and R. K. Hayashi, "Indenyl Rhenium Alkyne Complexes: CO Substitution via Alkyne-assisted Ring Slippage and CO-catalyzed Phosphine Substitution," *Organometallics* 22 (2003): 1183–1195, <https://doi.org/10.1021/om020884q>.
32. W. A. Herrmann, R. A. Fischer, W. Amslinger, and E. Herdtweck, "Alkin-Komplexe der Organorheniumoxide: Redox-Chemie und Nucleophilie der Oxo-Funktion von ( $\eta^5$ -Pentamethylcyclopentadienyl)( $\eta^2$ -diphenylethin)Oxorhenium(III)," *Journal of Organometallic Chemistry* 362 (1989): 333–343, [https://doi.org/10.1016/0022-328X\(89\)87255-9](https://doi.org/10.1016/0022-328X(89)87255-9).
33. C. R. Groom, I. J. Bruno, M. P. Lightfoot, and S. C. Ward, "The Cambridge Structural Database," *Acta Crystallographica Section B, Structural Science* 72 (2016): 171–179, <https://doi.org/10.1107/S2052520616003954>.
34. I. J. Bruno, J. C. Cole, P. R. Edgington, et al., "New Software for Searching the Cambridge Structural Database and Visualising Crystal Structures," *Acta Crystallographica Section B, Structural Science* 58 (2002): 389–397, <https://doi.org/10.1107/S0108768102003324>.
35. B. Kanellakopulos, B. Nuber, K. Raptis, and M. L. Ziegler, "Darstellung und Charakterisierung eines Technetium-Butadien-Komplexes; Röntgenstrukturanalyse von  $[\text{Tc}_2(\text{CO})_8][\mu\text{C}_4\text{H}_6]$ ," *Zeitschrift Fur Naturforschung Teil B Chemie, Biochemie, Biophysik, Biologie Und Verwandte Gebiete* 46 (1991): 55–59, <https://doi.org/10.1515/znb-1991-0112>.
36. F. A. Cotton, S. C. Haefner, and A. P. Sattelberger, "Metal–metal Multiplybonded Complexes of Technetium. 6. A  $\mu, \text{H}^1, \eta^2 \text{CH}_3\text{CN}$  Complex Prepared via Reductive Cleavage of the Electronrich  $\text{Tc} \equiv \text{Tc}$  Triple Bond in Decakisacetonitrile Ditechnetium Tetrafluoroborate," *Inorganica Chimica Acta* 266 (1997): 55–63, [https://doi.org/10.1016/S0020-1693\(97\)05533-3](https://doi.org/10.1016/S0020-1693(97)05533-3).
37. U. Abram and M. Roca Jungfer, "Cyclopentadienyl Complexes of Technetium," *Molecules (Basel, Switzerland)* 30 (2025): 4813, <https://doi.org/10.3390/molecules30244813>.
38. M. Benz, H. Braband, P. Schmutz, J. Halter, and R. Alberto, "From  $\text{Tc}^{\text{VII}}$  to  $\text{Tc}^{\text{I}}$ : Facile Syntheses of Bisarene Complexes  $[\text{99mTc}(\text{arene})_2]^+$  From Pertechnetate," *Chemical Science* 6 (2015): 165–169, <https://doi.org/10.1039/C4SC02461C>.
39. J. Cook, A. Davison, W. M. Davis, and A. G. Jones, "Insertion Chemistry of  $\text{HTc}(\text{CO})_3(\text{PPh}_3)_2$ ," *Organometallics* 14 (1995): 650–655, <https://doi.org/10.1021/om00002a012>.
40. I. Zolle, E. U. Heilmann, and W. McHugh, *Technetium-99m Pharmaceuticals. Preparation and Quality Control in Nuclear Medicine* (Springer, 2007), <https://doi.org/10.1007/978-3-540-33990-8>.
41. A. T. Taylor, M. Lipowska, L. Hansen, E. Malveaux, and L. G. Marzilli, " $^{99\text{m}}\text{Tc}$ MAEC complexes: New Renal Radiopharmaceuticals Combining Characteristics of  $^{99\text{m}}\text{TcMAG3}$  and  $^{99\text{m}}\text{TcEC}$ ," *Journal of Nuclear Medicine* 45 (2004): 885–886.
42. R. Alberto, R. Schibli, A. Egli, A. P. Schubiger, U. Abram, and T. A. Kaden, "A Novel Organometallic Aqua Complex of Technetium for the Labeling of Biomolecules: Synthesis of  $[\text{99mTc}(\text{OH}_2)_3(\text{CO})_3]^+$  From  $[\text{99mTcO}_4]^-$  in Aqueous Solution and Its Reaction With a Bifunctional Ligand," *Journal of the American Chemical Society* 120 (1998): 7987–7988, <https://doi.org/10.1021/ja980745t>.
43. M. Wenzel, "Tc-99m Labelling of Cymantrene Analogues With Different Substituents: A New Approach to Tc-99m Radiodiagnostics," *Journal of Labelled Compounds & Radiopharmaceuticals* 31 (1992): 641–650, <https://doi.org/10.1002/jlcr.2580310902>.
44. M. Wenzel and M. Saidi, "Brain Affinity of  $^{99\text{m}}\text{Tc}$ -labelled Esters of Cytectrene Carbonic Acid," *Journal of Labelled Compounds & Radiopharmaceuticals* 33 (1992): 77–80, <https://doi.org/10.1002/jlcr.2580330110>.
45. M. Wenzel, C. Klinge, and M. Saidi, "Tc-99m and Deuterium-marked, Brain-affine Radiodiagnostics: Comparison of HMPAO With Cytectrene Derivatives of Cyclic Amines," *Journal of Labelled Compounds & Radiopharmaceuticals* 33 (1993): 1030–1051, <https://doi.org/10.1002/jlcr.2580331107>.
46. D. Kuntschke, M. Wenzel, and P. Schulze, "New  $^{99\text{m}}\text{Tc}$ -cytectrene Amine Compounds as Specific Brain Imaging Agents," *Journal of Labelled Compounds & Radiopharmaceuticals* 36 (1994): 193–203, <https://doi.org/10.1002/jlcr.2580360212>.
47. T. W. Spradau and J. A. Katzenellenbogen, "Protein and Peptide Labeling With (cyclopentadienyl)Tricarbonyl Rhenium and Technetium," *Bioconjugate Chemistry* 9 (1998): 765–772, <https://doi.org/10.1021/bc980043t>.
48. T. W. Spradau, W. B. Edwards, C. J. Anderson, M. J. Welch, and J. A. Katzenellenbogen, "Synthesis and Biological Evaluation of Tc-99m-cyclopentadienyltricarbonyltechnetium-labeled Octreotide," *Nuclear Medicine and Biology* 26 (1999): 1–7, [https://doi.org/10.1016/S0969-8051\(98\)00060-2](https://doi.org/10.1016/S0969-8051(98)00060-2).
49. J. Wald, R. Alberto, K. Ortner, and L. A. Candrea, "Aqueous One-pot Synthesis of Derivatized Cyclopentadienyl-tricarbonyl Complexes of  $^{99\text{m}}\text{Tc}$  With an In Situ CO Source: Application to a Serotonergic Receptor Ligand," *Angewandte Chemie International Edition* 40 (2001): 3062–3066, [https://doi.org/10.1002/1521-3773\(20010817\)40:16%3c3062::AID-ANIE3062%3e3.0.CO;2-O](https://doi.org/10.1002/1521-3773(20010817)40:16%3c3062::AID-ANIE3062%3e3.0.CO;2-O).
50. J. Bernard, K. Ortner, B. Spingler, H. J. Pietzsch, and R. Alberto, "Aqueous Synthesis of Derivatized Cyclopentadienyl Complexes of Technetium and Rhenium Directed Toward Radiopharmaceutical Application," *Inorganic Chemistry* 42 (2003): 1014–1022, <https://doi.org/10.1021/ic0204575>.
51. C. L. Ferreira, C. B. Ewart, S. R. Bayly, et al., "Glucosamine Conjugates of Tricarbonylcyclopentadienyl Rhenium(I) and Technetium(I) Cores," *Inorganic Chemistry* 45 (2006): 6979–6987, <https://doi.org/10.1021/ic0605672>.
52. M. L. Bowen, Z. F. Chen, A. M. Roos, et al., "Longchain Rhenium and Technetium Glucosamine Conjugates," *Dalton Transactions* 2009 (2009): 9228, <https://doi.org/10.1039/b914309b>.
53. T. Uehara, T. Uemura, S. Hirabayashi, et al., "Technetium-99m labeled longchain Fatty Acid Analogues Metabolized by Boxidation in the Heart," *Journal of Medicinal Chemistry* 50 (2007): 543–549, <https://doi.org/10.1021/jm061017g>.
54. H. W. Peindy N'Dongo, P. D. Raposinho, C. Fernandes, et al., "Preparation and Biological Evaluation of Cyclopentadienylbased  $^{99\text{m}}\text{Tc}$ -complexes  $[(\text{CpR})^{99\text{m}}\text{Tc}(\text{CO})_3]$  Mimicking Benzamides for Malignant Melanoma Targeting," *Nuclear Medicine and Biology* 37 (2010): 255–264, <https://doi.org/10.1016/j.nucmedbio.2009.11.006>.
55. N. MalekSaied, R. El Aissi, S. Ladeira, and E. Benoist, "Synthesis and Biological Evaluation of a Novel  $^{99\text{m}}\text{Tc}$ -cyclopentadienyltricarbonyl Technetium Complex as a New Potential Brain Perfusion Imaging Agent," *Applied Organometallic Chemistry* 25 (2011): 680–686, <https://doi.org/10.1002/aoc.1827>.
56. Z. Li, M. Cui, J. Dai, et al., "Novel Cyclopentadienyl Tricarbonyl Complexes of  $^{99\text{m}}\text{Tc}$  Mimicking Chalcone as Potential SPECT Imaging Probes for Amyloid Plaques in Brain," *Journal of Medicinal Chemistry* 56 (2013): 471–482, <https://doi.org/10.1021/jm3014184>.
57. T. Dallagi, M. Saidi, A. Vessières, M. Huché, G. Jaouen, and S. Top, "Synthesis and Antiproliferative Evaluation of Ferrocenyl and Cymantrenyl Triarylbutene on Breast Cancer Cells. Biodistribution Study of the Corresponding technetium-99m Tamoxifen Conjugate," *Journal of Organometallic Chemistry* 734 (2013): 69–77, <https://doi.org/10.1016/j.jorganchem.2012.11.035>.
58. H. Zeng and H. Zhang, "Synthesis and Biological Evaluation of Fatty Acid Conjugates Bearing Cyclopentadienyl Donors Incorporated Into  $[\text{99mTc}/\text{Re}(\text{CO})_3]$  for Myocardial Imaging," *European Journal of Medicinal Chemistry* 72 (2014): 10–17, <https://doi.org/10.1016/j.ejmech.2013.11.015>.
59. S. Chen, Y. Zhang, X. Li, H. Jia, and J. Lu, "Evaluation of  $^{99\text{m}}\text{Tc}$  Cyclopentadienyl Tricarbonyl Triphenylphosphonium Cation for Multidrug Resistance," *Bioorganic & Medicinal Chemistry Letters* 27 (2017): 3551–3554, <https://doi.org/10.1016/j.bmcl.2017.05.053>.

60. X. Li, S. Chen, Z. Liu, Z. Zhao, and J. Lu, "Syntheses and Evaluations of Methoxymodified  $^{99m}\text{Tc}$  labeled Triphenylphosphonium Cations: Potential Radiometallic Probes for Multidrug Resistance Detection," *Journal of Organometallic Chemistry* 871 (2018): 28–35, <https://doi.org/10.1016/j.jorganchem.2018.07.003>.
61. M. Sagnou, B. Mavroidi, A. Shegani, et al., "Remarkable Brain Penetration of Cyclopentadienyl  $\text{M}(\text{CO})_3^+$  ( $\text{M} = ^{99m}\text{Tc}$ , Re) Derivatives of Benzothiazole and Benzimidazole: Diagnostic SPECT and Therapeutic Potential for Alzheimer's Disease," *Journal of Medicinal Chemistry* 62 (2019): 2638–2650, <https://doi.org/10.1021/acs.jmedchem.8b01949>.
62. H. Su and T. Chu, "Synthesis and Bioevaluation of Cyclopentadienyl Tricarbonyl technetium-99M 2-nitroimidazole Derivatives for Tumor Hypoxia Imaging," *Bioorganic & Medicinal Chemistry Letters* 60 (2022): 128583, <https://doi.org/10.1016/j.bmcl.2022.128583>.
63. R. Lengacher, S. Ott, O. Blacque, H. Braband, and R. Alberto, "A Multifunctional Tool: Cyclopentadienyl Re and  $^{99m}\text{Tc}$  Complex Synthesis on Highly Functionalised Arenes," *Journal of Organometallic Chemistry* 962 (2022): 122281, <https://doi.org/10.1016/j.jorganchem.2022.122281>.
64. Y. Liu, B. Spingler, P. Schmutz, and R. Alberto, "Metal-mediated retro-Diels–Alder of Dicyclopentadiene Derivatives: A Convenient Synthesis of  $[(\text{CpR})\text{M}(\text{CO})_3]$  ( $\text{M} = ^{99m}\text{Tc}$ , Re) Complexes," *Journal of the American Chemical Society* 130 (2008): 1554–1555, <https://doi.org/10.1021/ja0777411>.
65. H. W. Peindy N'Dongo, D. Can, B. Spingler, et al., "Aqueous Syntheses of  $[(\text{CpR})\text{M}(\text{CO})_3]$  ( $\text{M} = \text{Mn}$ ,  $^{99m}\text{Tc}$ , Re) Complexes With Bioactive Functionalities," *Journal of Organometallic Chemistry* 694 (2009): 981–987, <https://doi.org/10.1016/j.jorganchem.2008.12.006>.
66. D. Can, H. W. Peindy N'Dongo, B. Spingler, et al., "The  $[(\text{Cp})\text{M}(\text{CO})_3]$  ( $\text{M} = \text{Re}$ ,  $^{99m}\text{Tc}$ ) Building Block for Imaging Agents and Bioinorganic Probes: Perspectives and Limitations," *Chemistry Biodiversity* 9 (2012): 1849–1866, <https://doi.org/10.1002/cbdv.201200076>.
67. D. Can, P. Schmutz, S. Sulieman, B. Spingler, and R. Alberto, " $[(\text{CpR})\text{M}(\text{CO})_3]$  ( $\text{M} = \text{Re}$  or  $^{99m}\text{Tc}$ ) conjugates for Theranostic Receptor Targeting," *Chimia* 67 (2013): 267, <https://doi.org/10.2533/chimia.2013.267>.
68. Q. Nadeem, D. Can, Y. Shen, M. Felber, Z. Mahmood, and R. Alberto, "Synthesis of Tripeptidederivatized Cyclopentadienyl Complexes of Technetium and Rhenium as Radiopharmaceutical Probes," *Organic & Biomolecular Chemistry* 12 (2014): 1966, <https://doi.org/10.1039/c3ob41866a>.
69. S. Ursillo, D. Can, H. W. Peindy N'Dongo, P. Schmutz, B. Spingler, and R. Alberto, "Cyclopentadienyl Chemistry in Water: Synthesis and Properties of Bifunctionalized  $[(\eta^5\text{C}_5\text{H}_3\{\text{COOR}\}_2)\text{M}(\text{CO})_3]$  ( $\text{M} = \text{Re}$  and  $^{99m}\text{Tc}$ ) Complexes," *Organometallics* 33 (2014): 6945–6952, <https://doi.org/10.1021/om501029e>.
70. B. S. Frei and R. Alberto, "Multifunctional Cyclopentadienes as a Scaffold for Combinatorial Bioorganometallics in  $[(\eta^5\text{C}_5\text{H}_2\text{R}_1\text{R}_2\text{R}_3)\text{M}(\text{CO})_3]$  ( $\text{M} = \text{Re}$ ,  $^{99m}\text{Tc}$ ) Pianostool Complexes," *Chemistry– A European Journal* 24 (2018): 10156–10164, <https://doi.org/10.1002/chem.201801271>.
71. A. Frei, E. Fischer, B. C. Childs, J. P. Holland, and R. Alberto, "Two Is Better Than One: Difunctional High-affinity PSMA Probes Based on a  $[\text{CpM}(\text{CO})_3]$  ( $\text{M} = \text{Re}/^{99m}\text{Tc}$ ) Scaffold," *Dalton Transactions* 48 (2019): 14600–14605, <https://doi.org/10.1039/C9DT02506E>.
72. L. Eberle, S. Lindenthal, and J. Ballmann, "To Split or Not to Split:  $[\text{AsCCAs}]$ -Coordinated Mo, W, and Re Complexes and Their Reactivity Toward Molecular Dinitrogen," *Inorganic Chemistry* 63 (2024): 3682–3691, <https://doi.org/10.1021/acs.inorgchem.3c03244>.
73. L. Eberle, F. Kreis, C. A. M. Stein, J. M. Mörsdorf, and J. Ballmann, " $[\text{AsCCAs}]$ -coordinated Rhenium Hydrides and Their Reactivities Toward Unsaturated Hydrocarbons, Heterocumulenes, and  $\text{CO}_2$ ," *Inorganic Chemistry* 62 (2023): 8635–8646, <https://doi.org/10.1021/acs.inorgchem.3c00769>.
74. H. K. Wagner, H. Wadepohl, and J. Ballmann, "Molybdenum-mediated  $\text{N}_2$  Splitting and Functionalization in the Presence of a Coor-
75. K. Okamoto, Y. Omoto, H. Sano, and K. Ohe, "Alkyne-coordinating Tridentate Ligands: Structural Properties and Reactivity of Their Rhodium Complexes," *Dalton Transactions* 41 (2012): 10926, <https://doi.org/10.1039/c2dt31322g>.
76. K. Sasakura, K. Okamoto, and K. Ohe, "Incorporation of Monatomic Cations Onto an Ir–Ir Bond in a Dimeric Iridium(II) Complex Having a 1,3-diene-1,4-diyl Backbone," *Organometallics* 37 (2018): 2319–2324, <https://doi.org/10.1021/acs.organomet.8b00299>.
77. P. Federmann, T. Richter, H. Wadepohl, and J. Ballmann, "Synthesis and Reactivity of  $[\text{PCCP}]$ -Coordinated Group 5 Alkyl and Alkylidene Complexes Featuring a Metallacyclopentene Backbone," *Organometallics* 38 (2019): 4307–4318, <https://doi.org/10.1021/acs.organomet.9b00577>.
78. N. Liu, L. Liu, X. X. Zhong, F. B. Li, F. Y. Li, and H. M. Qin, "Ethynyl  $\Pi$ -coordinated and Noncoordinated Mononuclear Cu(I) Halide Diphosphine Complexes: Synthesis and Photophysical Studies," *New Journal of Chemistry* 46 (2022): 3236–3247, <https://doi.org/10.1039/D1NJ05578J>.
79. D. T. Gordon, R. L. Belaunzaran, R. E. Chafin, G. O. A. Yap, and M. M. Deegan, "Synthesis of an Isostructural Series of Group 6 Complexes Supported by an Alkyne based Pincer Ligand," *Organometallics* 44 (2025): 1296–1303, <https://doi.org/10.1021/acs.organomet.5c00113>.
80. B. Rudin, C. A. M. Stein, and J. Ballmann, "Tolanebased Phosphino and Arsinoruthenium Complexes in Three Different Oxidation States: Ru(I), Ru(II), and Ru(III)," *Chemistry– A European Journal* 31 (2025): e202404546, <https://doi.org/10.1002/chem.202404546>.
81. P. Federmann, H. K. Wagner, P. W. Antoni, et al., "Protected Diphosphadibenzo[a,e]pentalenones and Their Mono- and Dicationic P-bridged Ladder Stilbenes," *Organic Letters* 21 (2019): 2033–2038, <https://doi.org/10.1021/acs.orglett.9b00161>.
82. I. R. Fejes, G. P. A. Yap, and M. M. Deegan, "Ruthenium Coordination Chemistry of a Bisphosphine Alkyne Pincer Ligand," *European Journal of Inorganic Chemistry* 2025 (2025): e202500457, <https://doi.org/10.1002/ejic.202500457>.
83. B. Rudin, L. Eberle, and J. Ballmann, "2,2'-Diphosphino and 2,2'-Diarsenotolanes and Their Fe-, Co-, and Ni-complexes: Pnictogen-dependent Cyclization Tendencies and Metaldependent Stability and Reactivity Patterns," *Organometallics* 42 (2023): 933–943, <https://doi.org/10.1021/acs.organomet.3c00107>.
84. L. Eberle and J. Ballmann, "(Hetero)anilines From Dinitrogen via Nucleophilic Aromatic Substitution at Tungsten Nitrido Complexes," *Journal of the American Chemical Society* 147 (2025): 25123–25128, <https://doi.org/10.1021/jacs.5c06407>.
85. L. Eberle and J. Ballmann, "Synthesis of Collidine From Dinitrogen via a Tungsten Nitride," *Journal of the American Chemical Society* 146 (2024): 7979–7984, <https://doi.org/10.1021/jacs.4c02226>.
86. S. Senn, J.-M. Mörsdorf, M.-S. Bertrams, C. Kerzig, and J. Ballmann, " $\pi$  Extended Diphosphonium Bridged Ladder Stilbenes: Water Soluble Fluorophores With up to Eight Annulated Rings," *Chemical Science* 16 (2025): 20517–20526, <https://doi.org/10.1039/D5SC03752B>.
87. D. Balcells, O. Eisenstein, M. Tilset, and A. Nova, "Coordination and Insertion of Alkenes and Alkynes in Au(III) Complexes: Nature of the Intermediates From a Computational Perspective," *Dalton Transactions* 45 (2016): 5504–5513, <https://doi.org/10.1039/C5DT05014F>.
88. R. Stegmann, A. Neuhaus, and G. Frenking, "Theoretical Studies of Organometallic Compounds. 5. Alkyne and Vinylidene Complexes of Molybdenum and Tungsten in High-Oxidation States," *Journal of the American Chemical Society* 115 (1993): 11930–11938, <https://doi.org/10.1021/ja00078a035>.
89. K. Tatsumi, R. Hoffmann, and J. L. Templeton, "Structural and Theoretical Evidence for Participation of the Second Acetylene  $\Pi$ orbital in Transitionmetal Alkyne Complexes," *Inorganic Chemistry* 21 (1982): 466–468, <https://doi.org/10.1021/ic00131a095>.

90. J. L. Templeton and B. C. Ward, "Carbon13 Chemical Shifts of Alkyne Ligands as Variable Electron Donors in Monomeric Molybdenum and Tungsten Complexes," *Journal of the American Chemical Society* 102 (1980): 3288–3290, <https://doi.org/10.1021/ja00529a086>.
91. J. L. Templeton, "Fouerelectron Alkyne Ligands in Molybdenum(II) and Tungsten(II) Complexes," *Advances in Organometallic Chemistry* 29 (1980): 1–100, [https://doi.org/10.1016/S0065-3055\(08\)60352-4](https://doi.org/10.1016/S0065-3055(08)60352-4).
92. J. J. Carbó, P. Crochet, M. A. Esteruelas, et al., "Two and Fouerelectron Alkyne Ligands in Osmiumcyclopentadienyl Chemistry: Consequences of the  $\pi\perp\rightarrow M$  Interaction," *Organometallics* 21 (2002): 305–314, <https://doi.org/10.1021/om010645n>.
93. H. Nuss, N. Claiser, S. Pillet, et al., "A Comparative Study of the Topology of the Experimental Electron Density Within 2 and 4electron Donor Alkyne Complexes," *Dalton Transactions* 41 (2012): 6598, <https://doi.org/10.1039/c2dt30308f>.
94. M. Llunell, D. Casanova, J. Cirera, P. Alemany, and S. Alvarez, "version 2.1," (2013), [http://www.ee.ub.edu/index.php?option=com\\_jdownloads&-Itemid=529&view=viewcategory&catid=4](http://www.ee.ub.edu/index.php?option=com_jdownloads&-Itemid=529&view=viewcategory&catid=4).
95. M. Pinsky and D. Avnir, "Continuous Symmetry Measures. 5. The Classical Polyhedra," *Inorganic Chemistry* 37 (1998): 5575–5582, <https://doi.org/10.1021/ic980492s>.
96. S. Alvarez, D. Avnir, M. Llunell, and M. Pinsky, "Continuous Symmetry Maps and Shape Classification. The Case of Six-coordinated Metal Compounds," *New Journal of Chemistry* 26 (2002): 996–1009, <https://doi.org/10.1039/b200641n>.
97. D. Casanova, P. Alemany, J. M. Bofill, and S. Alvarez, "Shape and Symmetry of Heptacoordinate Transition-Metal Complexes: Structural Trends," *Chemistry– A European Journal* 9 (2003): 1281–1295, <https://doi.org/10.1002/chem.200390145>.
98. A. J. W. Thom, E. J. Sundstrom, and M. HeadGordon, "LOBA: A Localized Orbital Bonding Analysis to Calculate Oxidation States, With Application to a Model Wateroxidation Catalyst," *Physical Chemistry Chemical Physics* 11 (2009): 11297, <https://doi.org/10.1039/b915364k>.
99. M. Gimferrer, J. Van der Mynsbrugge, A. T. Bell, P. Salvador, and M. HeadGordon, "Facing the Challenges of Borderline Oxidationstate Assignments Using state-of-the-art Computational Methods," *Inorganic Chemistry* 59 (2020): 15410–15420, <https://doi.org/10.1021/acs.inorgchem.0c02405>.
100. I. F. Leach and J. E. M. N. Klein, "Oxidation States: Intrinsically Ambiguous?," *ACS Central Science* 10 (2024): 1406–1414, <https://doi.org/10.1021/acscentsci.4c00825>.
101. T. P. Curran, A. L. Grant, R. A. Lucht, J. C. Carter, and J. Affonso, " $\pi$ Ligands for Generating Transitionmetal–peptide Complexes: Coordination of Amino Acid Derivatives to Tungsten Utilizing Alkyne Ligands," *Organic Letters* 4 (2002): 2917–2920, <https://doi.org/10.1021/ol026298a>.
102. J. Baldas, J. F. Boas, J. Bonnyman, and G. A. Williams, "Studies of Technetium Complexes. Part 6. The Preparation, Characterisation, and Electron Spin Resonance Spectra of Salts of Tetrachloro and Tetrabromonitridotechnetate(VI): Crystal Structure of Tetraphenylarsonium Tetrachloronitridotechnetate(VI)," *Journal of the Chemical Society, Dalton Transactions* 1984 (1984): 2395, <https://doi.org/10.1039/dt9840002395>.
103. U. Mazzi, G. de Paoli, P. di Bernardo, and L. Magon, "Complexes of Technetium(IV) and (III) With Tertiary Phosphines," *Journal of Inorganic and Nuclear Chemistry* 38 (1976): 721–725, [https://doi.org/10.1016/0022-1902\(76\)80344-2](https://doi.org/10.1016/0022-1902(76)80344-2).
104. L. Krause, R. HerbstIrmer, G. M. Sheldrick, and D. Stalke, "Comparison of Silver and Molybdenum Microfocus Xray Sources for Singlecrystal Structure Determination," *Journal of Applied Crystallography* 48 (2015): 3–10, <https://doi.org/10.1107/S1600576714022985>.
105. G. M. Sheldrick, "SHELXT—integrated Spacegroup and Crystal structure Determination," *Foundations of Crystallography A* 71 (2015): 3–8, <https://doi.org/10.1107/S2053273314026370>.
106. G. M. Sheldrick, "Crystal Structure Refinement With SHELXL," *Foundations of Crystallography C* 71 (2015): 3–8, <https://doi.org/10.1107/S2053229614024218>.
107. APEX, APEX2, SMART, SAINT, SAINTPlus. Bruker AXS Inc., Madison, Wisconsin (USA), (2007).
108. C. F. Macrae, I. Sovago, S. J. Cottrell, et al., "Mercury 4.0: From Visualization to Analysis, Design and Prediction," *Journal of Applied Crystallography* 53 (2020): 226–235, <https://doi.org/10.1107/S1600576719014092>.
109. O. V. Dolomanov, L. J. Bourhis, R. J. Gildea, J. A. K. Howard, and H. Puschmann, "OLEX2: A Complete Structure Solution, Refinement and Analysis Program," *Journal of Applied Crystallography* 42 (2009): 339–341, <https://doi.org/10.1107/S0021889808042726>.
110. High performance computing (HPC) system Curta at Freie Universität Berlin.
111. M. J. Frisch, G. W. Trucks, H. B. Schlegel, et al., (2016), Gaussian 16, Revision B.01, Gaussian, Inc., Wallingford CT.
112. R. Dennington, T. A. Keith, and J. M. Millam, (2016), GaussView, Version 6, Semichem Inc., Shawnee Mission, KS.
113. M. D. Hanwell, D. E. Curtis, D. C. Lonie, C. Vandermeersch, E. Zurek, and G. R. Hutchison, "Avogadro: An Advanced Semantic Chemical Editor, Visualization, and Analysis Platform," *Journal of Cheminformatics* 4 (2012): 1–17, <https://doi.org/10.1186/1758-2946-4-17>.
114. S. Grimme, S. Ehrlich, and L. Goerigk, "Effect of the Damping Function in Dispersioncorrected Density Functional Theory," *Journal of Computational Chemistry* 32 (2011): 1456–1465, <https://doi.org/10.1002/jcc.21759>.
115. S. H. Vosko, L. Wilk, and M. Nusair, "Accurate Spin-dependent Electron Liquid Correlation Energies for Local Spin Density Calculations: A Critical Analysis," *Canadian Journal of Physics* 58 (1980): 1200–1211, <https://doi.org/10.1139/p80-159>.
116. A. D. Becke, "Density-functional Thermochemistry. III. The Role of Exact Exchange," *Journal of Chemical Physics* 98 (1993): 5648–5652, <https://doi.org/10.1063/1.464913>.
117. C. Lee, W. Yang, and R. G. Parr, "Development of the Colle-Salvetti Correlation-energy Formula Into a Functional of the Electron Density," *Physical Review B* 37 (1988): 785–789, <https://doi.org/10.1103/PhysRevB.37.785>.
118. F. Weigend and R. Ahlrichs, "Balanced Basis Sets of Split Valence, Triple Zeta Valence and Quadruple Zeta Valence Quality for H to Rn: Design and Assessment of Accuracy," *Physical Chemistry Chemical Physics* 7 (2005): 3297, <https://doi.org/10.1039/b508541a>.
119. K. A. Peterson, D. Figgen, E. Goll, H. Stoll, and M. Dolg, "Systematically Convergent Basis Sets With Relativistic Pseudopotentials. II. Small-core Pseudopotentials and Correlation Consistent Basis Sets for the Post-d Group 16–18 Elements," *Journal of Chemical Physics* 119 (2003): 11113–11123, <https://doi.org/10.1063/1.1622924>.
120. B. Metz, H. Stoll, and M. Dolg, "Small-core Multiconfiguration-Dirac–Hartree–Fock-adjusted Pseudopotentials for Post-d Main Group Elements: Application to PbH and PbO," *Journal of Chemical Physics* 113 (2000): 2563–2569, <https://doi.org/10.1063/1.1305880>.
121. K. L. Schuchardt, B. T. Didier, T. Elsethagen, et al., "Basis Set Exchange: A Community Database for Computational Sciences," *Journal of Chemical Information and Modeling* 47 (2007): 1045–1052, <https://doi.org/10.1021/ci600510j>.
122. T. Lu and F. Chen, "Multiwfn: A Multifunctional Wavefunction Analyzer," *Journal of Computational Chemistry* 33 (2012): 580–592, <https://doi.org/10.1002/jcc.22885>.
123. B. G. Janesko, K. B. Wiberg, G. Scalmani, and M. J. Frisch, "Electron Delocalization Range in Atoms and on Molecular Surfaces," *Journal of Chemical Theory and Computation* 12 (2016): 3185–3194, <https://doi.org/10.1021/acs.jctc.6b00343>.

124. B. G. Janesko, G. Scalmani, and M. J. Frisch, "Quantifying Solvated Electrons' delocalization," *Physical Chemistry Chemical Physics* 17 (2015): 18305–18317, <https://doi.org/10.1039/C5CP01967B>.
125. T. Liu and Q. Chen, "Interaction Region Indicator: A Simple Realspace Function Clearly Revealing Both Chemical Bonds and Weak Interactions," *Chemistry—Methods* 1 (2021): 231–239, <https://doi.org/10.1002/cmtd.202100007>.
126. R. F. W. Bader, *Atoms in Molecules: A Quantum Theory*; (Clarendon, Oxford, U.K 1990).
127. R. Hilal, S. G. Aziz, A. O. Alyoubi, and S. Elroby, "Quantum Topology of the Charge Density of Chemical Bonds. QTAIM Analysis of the C-Br and O-Br Bonds," *Procedia Computer Science* 51 (2015): 1872–1877, <https://doi.org/10.1016/j.procs.2015.05.423>.
128. C. S. López and A. R. de Lera, "Bond Ellipticity as a Measure of Electron Delocalization in Structure and Reactivity," *Current Organic Chemistry* 15 (2011): 3576–3593.
129. L. Zhang, F. Ying, W. Wu, P. C. Hiberty, and S. Shaik, "Topology of Electron Charge Density for Chemical Bonds From Valence Bond Theory: A Probe of Bonding Types," *Chemistry— A European Journal* 15 (2009): 2979–2989, <https://doi.org/10.1002/chem.200802134>.
130. W. Wang, B. Ji, and Y. Zhang, "Chalcogen Bond: A Sister Noncovalent Bond to Halogen Bond," *Journal of Physical Chemistry A* 113 (2009): 8132–8135, <https://doi.org/10.1021/jp904128b>.
131. J. A. Cabeza and J. F. van der Maelen, "García-Granda, S. Topological Analysis of the Electron Density in the N-Heterocyclic Carbene Triruthenium Cluster  $[\text{Ru}_3(\mu\text{-H})_2(\mu^3\text{-MeImCH}(\text{CO})_9)]$  (Me2Im = 1,3-dimethylimidazol-2-ylidene)," *Organometallics* 28 (2009): 3666–3672, <https://doi.org/10.1021/om9000617>.
132. E. Matito and M. Solà, "The Role of Electronic Delocalization in Transition Metal Complexes From the Electron Localization Function and the Quantum Theory of Atoms in Molecules Viewpoints," *Coordination Chemistry Reviews* 253 (2009): 647–665, <https://doi.org/10.1016/j.ccr.2008.10.003>, and references cited therein.
133. E. Matito, J. Poater, F. M. Bickelhaupt, and M. Solà, "Bonding in Methylalkalimetals  $(\text{CH}_3\text{M})_n$  (M = Li, Na, K;  $n = 1, 4$ ). Agreement and Divergences Between AIM and ELF Analyses," *Journal of Physical Chemistry B* 110 (2006): 7189–7198, <https://doi.org/10.1021/jp057517n>.
134. W. Humphrey, A. Dalke, and K. Schulten, "VMD: Visual Molecular Dynamics," *Journal of Molecular Graphics* 14 (1996): 33–38, [https://doi.org/10.1016/0263-7855\(96\)00018-5](https://doi.org/10.1016/0263-7855(96)00018-5).
135. F. Neese, "Software Update: The ORCA Program System, Version 6.0," *WIREs Computational Molecular Science* 15 (2025): e70019, <https://doi.org/10.1002/wcms.70019>.
136. D. Ganyushin and F. Neese, "First-principles Calculations of Zero-field Splitting Parameters," *Journal of Chemical Physics* 125 (2006): 024103, <https://doi.org/10.1063/1.2213976>.
137. G. L. Stoychev, A. A. Auer, and F. Neese, "Automatic Generation of Auxiliary Basis Sets," *Journal of Chemical Theory and Computation* 13 (2017): 554–562, <https://doi.org/10.1021/acs.jctc.6b01041>.
138. C. Kollmar, K. Sivalingam, B. Helmich-Paris, C. Angeli, and F. Neese, "A Perturbation-based Super-CI Approach for the Orbital Optimization of a CASSCF Wave Function," *Journal of Computational Chemistry* 40 (2019): 1463–1470, <https://doi.org/10.1002/jcc.25801>.
139. L. Lang and F. Neese, "Spin-dependent Properties in the Framework of the Dynamic Correlation Dressed Complete Active Space Method," *Journal of Chemical Physics* 150 (2019): 104104, <https://doi.org/10.1063/1.5085203>.
140. F. Neese, "The SHARK Integral Generation and Digestion System," *Journal of Computational Chemistry* 44 (2022): 381–396, <https://doi.org/10.1002/jcc.26942>.
141. M. Ugandi and M. Roemelt, "A Recursive Formulation of One-electron Coupling Coefficients for Spin-adapted Configuration Interaction Calculations Featuring Many Unpaired Electrons," *International Journal of Quantum Chemistry* 123 (2023): e27045, <https://doi.org/10.1002/qua.27045>.
142. F. Neese, "The ORCA Program System," *WIREs Computational Molecular Science* 2 (2012): 73–78, <https://doi.org/10.1002/wcms.81>.
143. F. Neese, "Software Update: The ORCA Program System, Version 4.0," *WIREs Computational Molecular Science* 8 (2018): 1–6, <https://doi.org/10.1002/wcms.1327>.
144. F. Neese, F. Wennmohs, U. Becker, and C. Riplinger, "The ORCA Quantum Chemistry Program Package," *Journal of Chemical Physics* 152 (2020): 224108, <https://doi.org/10.1063/5.0004608>.
145. F. Neese, "Software update: The ORCA program system—Version 5.0," *WIREs Computational Molecular Science* 12 (2022): e1606.
146. F. Neese, "Approximate Second-order SCF Convergence for Spin Unrestricted Wavefunctions," *Chemical Physics Letters* 325 (2000): 93–98, [https://doi.org/10.1016/S0009-2614\(00\)00662-X](https://doi.org/10.1016/S0009-2614(00)00662-X).
147. G. Knizia, "Intrinsic Atomic Orbitals: An Unbiased Bridge Between Quantum Theory and Chemical Concepts," *Journal of Chemical Theory and Computation* 9 (2013): 4834–4843, <https://doi.org/10.1021/ct400687b>.
148. G. Knizia and J. E. M. N. Klein, "Electron Flow in Reaction Mechanisms — revealed From First Principles," *Angewandte Chemie International Edition* 54 (2015): 5518–5522, <https://doi.org/10.1002/anie.201410637>.
149. D. Andrae, U. Häußermann, M. Dolg, H. Stoll, and H. Preuß, "Energy-adjusted Ab Initio Pseudopotentials for the Second and Third Row Transition Elements," *Theoretica Chimica Acta* 77 (1990): 123–141, <https://doi.org/10.1007/BF01114537>.
150. F. Weigend, F. Furche, and R. Ahlrichs, "Gaussian Basis Sets of Quadruplezeta Valence Quality for Atoms H–Kr," *Journal of Chemical Physics* 119 (2003): 12753–12762, <https://doi.org/10.1063/1.1627293>.

## Supporting Information

Additional supporting information can be found online in the Supporting Information section.

**Supporting File 1:** Experimental details (S1), Crystallographic data (S2), Spectral data (S3), Computational data (S4), Additional figures and explanatory text (S5), an excel sheet containing tabular information about the literature surveys and compact calculation information and crystallographic information files (CIF/CheckCIF) are provided as **Supporting Information**. All data are available in the main text or the supplementary materials. CCDC 2521631 to CCDC 2521634 and CCDC 2521636 to CCDC 2521640 contain the supplementary crystallographic data for this paper. The data can be obtained free of charge from The Cambridge Crystallographic Data Centre via [www.ccdc.cam.ac.uk/structures](http://www.ccdc.cam.ac.uk/structures). Original data (e.g., spectra files) are available through reasonable requests by contacting the corresponding author. The procedures for the preparation of all materials are contained in the Supporting Information. The authors have cited additional references within the Supporting Information [103–150].

**Supporting File 2:** anie72357-sup-0002-Data.zip.